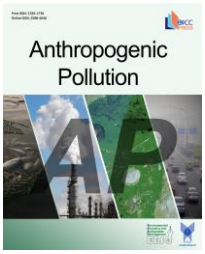

J. Anthropog Pollut 2025; 9(2): Article 18

Anthropogenic Pollution (AP)

https://doi.org/10.57647/J.AP.2025.0902.18

Research Article

Enhancing Soil Remediation: Integrated *Mycobacterium* and Barley (*Hordeum Vulgare*) Systems for Petroleum Hydrocarbons and Heavy Metals Restoration in Soils Near Shiraz Oil Refinery

Maryam Aghakhani[1], Seyed Ali Abtahi[1,*], Davood Azadi[2,*], Mojtaba Jafarinia[3]

[1] *Department of Soil Science, Marv.C., Islamic Azad University, Marvdasht, Iran*
[2] *Department of Microbiology, School of Medicine, Baqiyatallah University of Medical Sciences, Tehran, Iran.*
[3] *Department of Biology, Marv.C., Islamic Azad University, Marvdasht, Iran*

***Corresponding author:** Seyedaliabtahi@yahoo.com

Article History:

Received:
01 June 2025

Revised:
20 July 2025

Accepted:
31 August 2025

Published in Issue:
31 December 2025

Abstract

Industrial activities, particularly oil refining, release significant pollutants like TPH, PAHs, and heavy metals into the environment, necessitating sustainable remediation strategies. Therefore, in this study we evaluated the synergistic potential of bioremediation using *Mycobacterium* and phytoremediation with barley to remediate contaminated soils in Shiraz oil refinery, Iran. 36 soil samples were analyzed to isolate bioremediating mycobacteria using turbidometric, chromatographic, biochemical, and molecular assays. Greenhouse experiments used soil spiked with PAHs (100–200 mg/kg)and heavy metals (As, Hg, Cd, Pb, Cr; 3–400 mg/kg) at low, medium, and high levels. Five treatments include control, phytoremediation(P),bioremediation(B),combined phytoremediation and bioremediation(MB),and sterile control, were assessed over 90 days, analyzing soil properties, contaminant levels, plant growth, TF, and BAF.13 *Mycobacterium* isolates (36.11%)representing nine species were identified. Key species such as *M. gilvum* and *M. smegmatis* achieved >60% degradation of both PAHs and heavy metals, while *M. austroafricanum* and *M. vaccae* showed superior PAH degradation (65–80%),with *M. vaccae* also achieving 75% heavy metal reduction. The MB treatment significantly outperformed the others, achieving 78–86% PAH degradation and 58–68% heavy metal removal ($p < 0.001$). Soil quality indicators improved notably: microbial biomass increased by 35%, pH rose from 5.8 to 6.8, organic matter increased from 2.0% to3.5%, and EC decreased from 1.5 to 1.0 dS/m. Barley biomass increased by 25%(roots)and 20% (shoots), with TF and BAF values ranging from 0.25–0.55. This study demonstrates that integrated bioremediation using barley and Mycobacteriaoffers a sustainable strategy for restoring petroleum and heavy metal contaminated soils in industrial areas.

Keywords: Soil Recovery; Environmental Restoration; Ecological Innovation; Bioremediation; Phytoremediation; 16SrRNA

Cite this article: Aghakhani M., Abtahi S. A., Azadi D., Jafarinia M., (2025). *Enhancing soil remediation:* Integrated *Mycobacterium* and barley (*Hordeum vulgare*) systems for petroleum hydrocarbons and heavy metals restoration in soils near Shiraz Oil Refinery. *Journal Anthropog Pollut, 9(2),* Article 18. https://doi.org/10.57647/J.AP.2025.0902.18

1. Introduction

Oil refineries and industrial activities worldwide are major sources of soil contamination, releasing persistent pollutants such as total petroleum hydrocarbons (TPH), polycyclic aromatic hydrocarbons (PAHs), and potentially toxic elements (PTEs) including lead (Pb), cadmium (Cd), arsenic (As), mercury (Hg), and chromium (Cr). These contaminants, originating from crude oil processing, industrial discharges, and atmospheric deposition, severely degrade soil quality by altering its physical structure, reducing water retention, and inhibiting nutrient cycling (Elmi et al., 2021 ; Jin et al., 2020). The United Nations Environment Programmer (UNEP) estimates that over 5 million sites globally are affected, with more than 1.5 million hectares of land contaminated annually, particularly in industrial zones (Biswas et al., 2015, Nádudvari et al., 2021). The World Health Organization (WHO) reports that soil pollution contributes to over 200,000 deaths yearly due to associated health risks, such as a 20–30% increased risk of lung and skin cancer, neurological disorders, and respiratory issues in exposed populations (Stepanova et al., 2019 ; Munzel et al., 2023) . Additionally, these pollutants diminish microbial diversity and soil fertility, disrupting ecosystem services such as pollination and carbon sequestration, with a reported 10–15% decline in microbial biomass in contaminated sites (Ravanbakhsh et al., 2023). Conventional remediation techniques, including chemical oxidation, thermal desorption, and soil excavation, address these issues but are costly, ranging from $50 to $500 per ton of soil treated, and often generate secondary pollutants like greenhouse gases or toxic byproducts (Grifoni et al., 2022).This has driven interest in sustainable alternatives such as bioremediation and phytoremediation (Afshar et al., 2022 ; Gooran Ourimi and Nezhadnaderi, 2020). Bioremediation is a process that employs microorganisms to degrade or remove contaminants from the environment, offering a cost-effective solution (ranging from $10 to $50 per ton) with minimal site disruption (Motallebirad et al., 2023, Hosseini et al., 2023). Among these microorganisms, Mycobacterium spp. stand out due to their possession of unique enzymatic systems, such as dioxygenases, which enable the degradation of complex polycyclic aromatic hydrocarbons (PAHs) by up to 80% within 6 days. Their ability to form biofilms and tolerate harsh contaminated conditions further enhances their efficacy in hydrocarbon degradation (Azadi et al., 2017). Some plants have the ability to contribute to reducing soil contamination from heavy elements (Hosseinzadeh et al., 2024 ; Talkhoncheh and Rouzbahani, 2024). Phytoremediation, conversely, utilizes plants such as barley (*Hordeum vulgare*), a resilient cereal crop with a deep root system extending up to 40 cm, to extract, stabilize, or degrade pollutants while increasing soil organic matter by 15–20% (Vasilachi et al., 2023). The integration of these methods creates a synergistic effect, enhancing pollutant removal and soil restoration, as evidenced by a Rhizobium-alfalfa system achieving 85% PAH reduction over 120 days (Holatko et al., 2024).

In Iran, environmental pollution is a pressing concern, with the oil refinery and other industrial zones contributing to soil contamination levels exceeding 8,000 mg/kg TPH and 100 mg/kg potentially toxic elements in some areas (Shahab-Deljoo et al., 2023). This has led to a 20% decline in local agricultural productivity and a 10% reduction in soil microbial diversity, threatening ecosystem stability and food security (Azadi et al., 2017). The lack of integrated remediation strategies in such contexts underscores the need for innovative solutions tailored to Iran's environmental challenges. Consequently, we hypothesized that integrating *Mycobacterium*-mediated bioremediation with barley phytoremediation would significantly enhance the degradation of petroleum hydrocarbons and immobilization of heavy metals in soils near the Shiraz oil refinery. Therefore, in this study sought to test this hypothesis by evaluating the combined approach to devise a sustainable remediation strategy that restored soil health and promoted long-term ecosystem recovery in Iran's industrially affected areas.

2. Materials and Methods

2.1. Soil sampling and bacterial screening

From March 2024 to July 2024 in a cross sectional study, a total number of 36 soil samples (15–30 g of soil per replicate, and three replicates were taken per site to account for spatial variability. Samples were collected at a depth of 0–20 cm using a stainless-steel auger, stored in sterile polyethylene bags, and transported to the laboratory within 24 hours.) collected from eight polluted sites from lands around Shiraz oil refinery and transferred directly to the microbiology laboratory at Islamic Azad University, Marvdasht Branch, for further analysis. The samples were processed based on standard procedures. In summary, five grams of soil was transferred to 50 ml sterile centrifuge tube. Then, 20 ml sterile distilled water was added to the tube and vortexed for 5 min, and centrifuged at 5000×g (Universal HB320, Iran) at room temperature for 15 min. Following centrifugation, both the supernatant and pellet were processed as follow to enhance the isolation of a

broader range of bioremediation-capable microorganisms, including those that might otherwise be overlooked or lost during processing. The supernatant and pellet were decontaminated in separate tubes by 1% NaOH applied separately to adjust the pH and facilitate cell lysis, followed by 3% sodium lauryl sulfate used independently as a surfactant to enhance microbial release from soil particle. Afterwards, 100 µL of the decontaminated sample was inoculated into the Sauton's medium (supplemented with antibacterial and antifungal antibiotics including kanamycin (50 µg/ml), nystatin (50 µg/ml) and nalidixic acid (50 µg/ml) and Löwenstein–Jensen (LJ) (To selectively eliminate non-Mycobacterial microorganisms, including saprophytes, fungi, and other contaminating bacteria) and were incubated at 25 °C, 30 °C and 35 °C with 5% CO_2 atmosphere for 8 weeks. Subsequently, the pellet was treated with NaOH (Azadi et al., 2017).

2.2. Identification of *Mycobacterium* Species

The isolates grown on media, initially were characterized phenotypically by the use of conventional phenotypic and biochemical tests. The tests included acid-fast staining, colony characterization, the growth rate at 25°C, 32°C, 37°C and 42°C, and standard biochemical assays such as semi quantitative and heat-stable (68°C) catalase production, tween opacity, pigment production, urease activity, nitrate reduction, tellurite reduction, niacin accumulation, and pyrazinamidase (Siavashifar et al., 2021). Chromosomal DNA of *Mycobacterium* isolates was extracted using boiling method described by Azadi et al. (Azadi et al., 2020). Genus- and species-level identification was performed using PCR amplification and direct sequencing of the full-length 16S rRNA gene. Sequencing was performed in Pishgam Biotech Company (Iran) (Azadi et al., 2020). The sequences were aligned manually and compared and analyzed with all sequences of the closely related *Mycobacterium* species retrieved from GenBank database using jPhydit program version 1.1.3 (Jeon et al., 2005). The relationship between our isolates and the standard stablished *Mycobacterium* species was depicted by using a high bootstrap value phylogenetic tree of 16S rRNA gene by MEGA X software, using the neighbor-joining method with arithmetic mean of pair wise differences matrix.

2.3. Soil physicochemical and microbial analysis

Surface soils (0–30 cm depth) were homogenized, air-dried, and sieved (<2 mm) to ensure uniformity. Initial contaminant concentrations were determined using gas chromatography-mass spectrometry (GC-MS; Agilent 7890B, USA) for PAHs following EPA Method 8270D, and atomic absorption spectrometry (AAS; PinAAcle 900T, USA) for potentially toxic elements after aqua regia digestion, per EPA Method 6020B (Ekanem et al., 2021, Kanwar et al., 2020). Soil physicochemical properties were analyzed according to standard protocols (Sparks et al., 1998). Moisture content was measured gravimetrically by drying samples at 105°C for 24 hours. Soil pH and electrical conductivity (EC) were assessed in a 1:5 soil: water slurry using a Hanna HI9813 device (USA). Total carbon was determined by dry combustion with an Elementar Vario EL III analyzer (Germany). Available potassium (K) was extracted using the ammonium acetate method and quantified via flame photometry (Jenway PFP7, UK), while available phosphorus (P) was extracted using the Olsen method and measured by spectrophotometry (Shimadzu UV-1800, Japan). Soil texture was determined using the hydrometer method (Singh et al., 2022). For identification of the normal soil microbiota, soil suspensions (5 g soil in 20 mL sterile distilled water, vortexed for 5 minutes) were inoculated onto MacConkey agar and blood agar. Cultures were incubated at 37°C for 24–48 hours under aerobic conditions. Representative colonies were selected based on morphology and further identified using the API 20 system (bioMérieux, France), (Masi et al., 2021). The detailed physicochemical, contaminant, and microbial profiles of the soil samples are presented in Table 1.

2.4. Biodegradation Assessment

The bioremediation capacity of the identified *Mycobacterium* isolated in this study was assessed based on method described by Kanaly et al (2000) (Kanaly and Harayama, 2000) . The details are as follow:

2.5. Chemicals and media

A PAHs mixture containing phenanthrene, pyrene, anthracene, and fluoranthene (AccuStandard, Spain) was prepared at 0.2 mg/mL in a 1:1 solution of dichloromethane and methanol (Merck, Germany). Stock solutions of potentially toxic elements (Cr, Pb, Hg, Cd, Cu and AS Sigma-Aldrich, USA) were prepared at 10 mg/mL in deionized water. A Mineral Salt Medium (MSM) was used for bioremediation experiments, consisting of the following per liter: 0.25 g $MgSO_4 \cdot 7H_2O$, 0.5 g KH_2PO_4, 0.5 g K_2HPO_4, 1 g NaCl, 0.009 g $CaCl_2 \cdot 2H_2O$, 0.5 g KNO_3, 0.1 g $MnCl_2 \cdot 4H_2O$, 0.07 g $ZnCl_2$, 0.015 g $CuCl_2 \cdot 2H_2O$, 0.025 g $NiCl_2 \cdot 6H_2O$, 0.12 g $CoCl_2 \cdot 6H_2O$, and 0.025 g $Na_2MoO_4 \cdot 2H_2O$ (Merck, Germany). The MSM was autoclaved at 121°C for 15 minutes (Tomy SX-500, Japan) prior to use.

2.6. Bioremediation capability assessment

The bioremediation potential of the *Mycobacterium* isolates was assessed by inoculating 1 mL of a 0.5 McFarland turbidity suspension (1×10^8 CFU/mL) into 100 mL of MSM supplemented with 1% PAHs and 1% heavy metal mixture (50 mg/L) in 250 mL Erlenmeyer flasks. The flasks were incubated at 30°C for 14 days on an orbital shaker (Arta 55SIN, Iran) at 90 ×g. Bacterial growth was monitored daily by measuring optical density (OD) at 560 nm using a spectrophotometer (Shimadzu UV-1800, Japan). An increase in OD indicated microbial growth and potential pollutant degradation. After 6 days, 5 mL samples were analyzed for petroleum hydrocarbon and heavy metal degradation using GC-MS and AAS, respectively.

Determination of PAHs degradation: For PAHsanalysis, 5 mL of MSM was transferred to screw-cap glass tubes, and 0.6 mL of tetrachloroethylene: methanol (1:100, Merck, Germany) was added as the extraction solvent. Samples were vortexed for 10 seconds, centrifuged at 3000 ×g for 10 minutes (Universal HB320, Iran), and the organic phase was analyzed via GC-MS (Agilent 7890B, USA) using an HP-5MS column (30 m × 0.25 mm, 0.25 µm film thickness, Agilent, USA). The oven temperature increased from 60°C (held for 2 minutes) to 280°C at 10°C/min, held for 10 minutes, with helium (Air Liquide, France) as the carrier gas at 1 mL/min. The injector was set at 250°C in splitless mode, and the mass spectrometer operated in EI mode at 70 eV. Hydrocarbons were identified and quantified using retention times, mass spectra, and calibration curves from standards, with degradation efficiency calculated by comparing residual concentrations to initial levels (Ekanem et al., 2021).

Determination of heavy metal degradation: For heavy metal analysis, 5 mL of MSM was transferred to screw-cap glass tubes, and 0.6 mL of aqua regia (HNO_3: HCl, 3:1, Merck, Germany) was added. Samples were digested at 95°C for 30 minutes in a water bath, cooled, filtered through a 0.45 µm membrane filter (Millipore, USA), and diluted for analysis. Heavy metal concentrations (Cr, Pb, Cd, Cu) were measured using AAS (PerkinElmer AAnalyst 400, USA) and compared to a control MSM without bacterial inoculation to determine biosorption or degradation efficiency (Kanwar et al., 2020).

Bioremediation efficiency assessment: The efficiency of bioremediation was evaluated by monitoring the degradation of PAHs and the reduction of heavy metal concentrations in each experimental flask. PAH concentrations were quantified using GC-MS, while heavy metal levels were determined through AAS. Samples were collected at predetermined intervals (0, 3, 7, 10, and 14 days) to assess the temporal progression of contaminant removal. Biodegradation efficiency was calculated by comparing the measured concentrations of PAHs and potentially toxic elements at each time point to their respective initial levels, expressed as percentage reduction concentrations (Wu et al., 2017, Kanwar et al., 2020).

2.7. Analysis of synergisticeffects of bioremediation and phytoremediation

A greenhouse experiment was conducted using a factorial design with three replicates per treatment, resulting in a total of 15 experimental units (5 treatments × 3 concentrations × 3 replicates = 45 experimental units). The experiment comprised five treatments: (1) control (unamended contaminated soil), (2) phytoremediation (PB) (barley only), (3) bioremediation (B) (bacterial consortium of five *Mycobacterium* strains: *M. gilvum*, *M. vaccae*, *M. austroafricanum*, *M. houstonense*, and *M. franklinii*), (4) combined phytoremediation and bioremediation (MB) (barley + bacterial consortium), and (5) sterile control (autoclaved contaminated soil). Each treatment was applied at three contamination levels (low, medium, high), with three replicates per treatment-concentration combination, resulting in. The experiment was carried out in 45 polyethylene pots (25 cm diameter, 30 cm height, 10 kg capacity), each filled with 4 kg of soil collected from an uncontaminated agricultural field in Marvdasht, Fars Province, Iran (30°03'N, 52°48'E). The soil, classified as a sandy loam, was air-dried, sieved to <2 mm using Atlas standard sieves (Iran), and characterized for baseline physicochemical properties following Sparks et al. (1998). Soil was artificially contaminated by spiking with a mixture of polycyclic aromatic hydrocarbons (PAHs; phenanthrene, pyrene) at three concentrations: low (50 mg/kg), medium (100 mg/kg), and high (150 mg/kg), and potentially toxic elements (As, Hg, Cd, Pb, Cr) at three concentrations: low (5 mg/kg), medium (10 mg/kg), and high (15 mg/kg), following EPA Method 3550C for spiking procedures. The spiked soil was homogenized and aged for 30 days at 25°C in the dark to stabilize contaminants and simulate field conditions, with periodic mixing to ensure uniformity. Mean values for each treatment-concentration combination were calculated from the three replicates to assess remediation efficacy.

For the phytoremediation treatment, barley seeds were sown at a density of three seeds per pot and thinned to one plant per pot after 7 days of germination. For the bioremediation treatment, a consortium of five *Nocardia* strains (*M. gilvum, M. vaccae, M. austroafricanum, M. houstonense, and M. franklinii*), previously identified for their superior PAH degradation and heavy metal tolerance was prepared as a 0.5 McFarland suspension (1×10^8 CFU/mL per strain, total 5×10^8 CFU/g soil) in sterile 0.85% saline. Each pot in the bioremediation and combined

treatments received 100 mL of the bacterial consortium, applied by surface drenching to ensure even distribution. The control and phytoremediation treatments received equivalent volumes of sterile saline to maintain consistent moisture levels.

Pots were maintained in a greenhouse at 25±2°C, 60% water-holding capacity (adjusted biweekly using deionized water), and a 16:8 h light: dark cycle (400 µmol/m²/s photosynthetically active radiation). The experiment ran for 90 days, with pots randomized weekly to minimize positional effects. Soil moisture, temperature, and plant health were monitored daily. Soil samples were collected before and after the experiment to assess the physicochemical properties and contaminant levels. Initial and final soil analyses encompassed pH, EC, OC, TN, available P, K, potentially toxic elements and PAHs were analyzed respectively, as described earlier.

2.8. Analysis of Translocation Factor (TF) and Bioaccumulation Factor (BAF) of heavy metal in barley

Post-harvest, barley shoots and roots were oven-dried at 70°C for 48 hours, digested with HNO_3-$HClO_4$ (3:1 v/v), and analyzed for metal concentrations using atomic absorption spectroscopy (AAS, PerkinElmer 700, USA). Soil samples were similarly digested and analyzed. TF was calculated as the ratio of metal concentration in shoots to roots (metal_shoot/metal_root), and BAF as the ratio of metal concentration in shoots to soil (metal_shoot/metal_soil) (Agarwal et al., 2022).

2.9. Quality Control and Quality Assurance (QC/QA)

To ensure the accuracy, precision, and reproducibility of the analytical results, rigorous QC and QA protocols were implemented throughout the study. All analytical procedures, including soil contaminant quantification and microbial enumeration, were conducted in triplicate to assess intra-laboratory variability, with acceptance criteria set at a relative standard deviation (RSD) of less than 10%, consistent with guidelines from similar bioremediation studies (Hosseini et al., 2023).

Calibration curves for TPH and heavy metal analysis were prepared using certified reference materials (CRMs) from the National Institute of Standards and Technology (NIST), with correlation coefficients (R^2) exceeding 0.99 to validate instrument performance. Blank samples and spiked controls were analyzed with each batch to monitor contamination and recovery rates, achieving recovery efficiencies of 90–105% for PAHs and 85–100% for heavy metals, aligning with QA standards reported by Kanwar et al. (2020).

Instrument calibration was performed daily, and method detection limits (MDLs) were determined as three times the standard deviation of blank measurements, ensuring sensitivity (e.g., MDL for PAHs: 0.1 mg/kg; heavy metals: 0.05 mg/kg). Additionally, inter-laboratory comparison was conducted by sending 10% of samples to an accredited external laboratory, with results agreeing within ±5%, confirming data integrity.

2.10. Statistical Analysis

For the analysis of the data, a one-way ANOVA was employed, followed by the comparison of means using Duncan's Multiple Range Test (DMRT). Prior to the execution of ANOVA, the Kolmogorov-Smirnov test was administered to confirm the normality of the data, while Levene's test was conducted to ensure the homogeneity of variances. The entirety of the data analysis was meticulously performed utilizing SAS software (version 9.4, SAS Institute Inc., Cary, NC).

3. Results

The contaminated soils from eight sampling sites in Marvdasht, Iran, comprised Aridisols, Mollisols, and Alfisols. Soil properties revealed a mean pH of 6.9 ± 0.001, electrical conductivity (EC) ranging from 98.3 to 145 mS (mean 122 ± 0.011 mS), and organic carbon varying from 0.12% to 6.0% (mean 1.8 ± 0.00002%). Available potassium and phosphorus levels ranged from 25 to 268 ppm (mean 225 ± 4.167 ppm) and 0.1 to 32 ppm (mean 9.1 ± 0.003 ppm), respectively, while total nitrogen varied from 24 to 78 mg/L (mean 49 ± 0.222 mg/L). Total petroleum hydrocarbon (TPH) concentrations ranged from 120 to 8,500 mg/kg, with the highest levels (mean 7,200 mg/kg) observed in soils adjacent to oil refinery discharge sites (Sites 6–8). Total polycyclic aromatic hydrocarbon (PAH) levels ranged from 10 to 350 mg/kg, predominantly high-molecular-weight compounds. Heavy metal concentrations included lead (15–120 mg/kg), cadmium (0.5–5 mg/kg), chromium (50–300 mg/kg), and nickel (40–200 mg/kg. Microbial populations, assessed as colony-forming units (CFU), ranged from 1.0 × 10^4 to 2.0 × 10^6 CFU/g soil, reflecting a diverse soil microflora including *Bacillus* spp., *Clostridium* spp., *Streptomyces* spp., *Rhodococcus* spp., *Pseudomonas* spp., *Klebsiella* spp., *Burkholderia* spp., *Aspergillus* spp., *Penicillium* spp., and *Fusarium* spp., indicating substantial bioremediation potential (Table 1).

3.1. Isolation and identification of *Mycobacterium* Species

From 36 soil samples collected around the Shiraz oil refinery in Fars Province, Iran, 13 *Mycobacterium* isolates (36.11%) belonging to nine species were identified through culture, morphological, biochemical, and 16S rRNA gene sequence analyses. All 36 samples (100%) were contaminated with Gram-positive and Gram-negative bacteria and fungi, with *Mycobacterium* isolates detected in 8 samples (22.22%) from farmland sites; no *Mycobacterium* was found in samples from other sites. Of the 13 isolates, 2 were slow-growing (with an extended helix) and 11 were rapid-growing (with a short helix 18 at positions 451–482), all classified in Runyon Group IV. The identified species included *M. austroafricanum* (3 isolates, 23.07%), *M. chubuense* and *M. celeriflavum* (2 isolates each, 15.38%), and *M. gilvum*, *M. smegmatis*, *M. vanbaalenii*, *M. vaccae*, *M. houstonense*, and *M. franklinii* (1 isolate each, 7.7%). Phenotypic, biochemical, and molecular profiles of the isolates are detailed in Table 2. The 16S rRNA gene sequences were deposited in GenBank under accession numbers: *M. austroafricanum* (AM1: PQ373912), *M. chubuense* (AM5: PQ373941), *M. celeriflavum* (AM7: PQ374834), *M. gilvum* (AM8: PQ374042), *M. smegmatis* (AM9: PQ374126), *M. vaccae* (AM10: PQ374140), *M. houstonense* (AM11: PQ374170), *M. franklinii* (AM12: PQ374179), and *M. vanbaalenii* (AM13: PQ374202).

Phylogenetic relationships with established *Mycobacterium* species were supported by high bootstrap values in a tree constructed using MEGA X software via the neighbor-joining method with an arithmetic mean of pairwise differences matrix (Figure 1).

Table 1. Details of sampling site, physical and chemical properties, and microflora of collected soil samples and mean values of soil parameters

Site	Number of Samples	Soil Type	CFU Range (per gram)	Soil Microflora	K (ppm)	P (ppm)	pH	EC (mS)	Organic Carbon (%)	Total Nitrogen (mg/L)	TPH (mg/kg)	Total PAHs (mg/kg)	Potentially toxic elements (mg/kg)
1	5	Mollisols	1.0×10^4 - 5.0×10^4	*B. subtilis, C. sporogenes, A. globiformis, P. putida, K. oxytoca, P. vulgaris, A. niger, P. chrysogenum, C. tropicalis*	252	0.5	6.4	120.9	3.4	35	120	10	Pb: 15, Cd: 0.5, Cr: 50, Ni: 40
2	5	Mollisols	5.0×10^4 - 1.0×10^5	*B. licheniformis, S. coelicolor, P. polymyxa, P. aeruginosa, E. coli, A. calcoaceticus, F. solani, P. verrucosum, R. stolonifer*	234	11	7.2	118	1.6	43	500	50	Pb: 30, Cd: 1.0, Cr: 75, Ni: 60
3	5	Aridisols	1.0×10^5 - 2.5×10^5	*B. megaterium, C. perfringens, M. chalcea, S. marcescens, P. fluorescens, B. cepacia, A. terreus, F. oxysporum, P. digitatum*	196	8	6.2	131.6	0.2	75	1,200	100	Pb: 50, Cd: 2.0, Cr: 100, Ni: 80

Table 1. Details of sampling site, physical and chemical properties, and microflora of collected soil samples and mean values of soil parameters (continued)

Site	Number of Samples	Soil Type	CFU Range (per gram)	Soil Microflora	K (ppm)	P (ppm)	pH	EC (mS)	Organic Carbon (%)	Total Nitrogen (mg/L)	TPH (mg/kg)	Total PAHs (mg/kg)	Potentially toxic elements (mg/kg)
4	4	Mollisols	2.5×10^5 - 5.0×10^5	*B. cereus, T. vulgaris, P. macerans, K. pneumoniae, P. mirabilis, P. stutzeri, A. fumigatus, P. expansum, R. oryzae*	268	0.7	7.3	124	0.23	25	3,000	150	Pb: 70, Cd: 3.0, Cr: 150, Ni: 100
5	4	Aridisols	5.0×10^5 - 7.5×10^5	*B. thuringiensis, N. asteroides, S. griseus, E. coli, B. pseudomallei, A. baumannii, C. albicans, A. flavus, M. indicus*	25	0.1	6.8	118.3	0.12	24	5,000	200	Pb: 90, Cd: 4.0, Cr: 200, Ni: 150
6	4	Alfisols	7.5×10^5 - 1.0×10^6	*B. subtilis, C. tetani, R. erythropolis, P. syringae, K. oxytoca, S. liquefaciens, P. notatum, T. harzianum, F. verticillioides*	214	32	7.9	145	6.0	65	7,200	250	Pb: 100, Cd: 4.5, Cr: 250, Ni: 180
7	5	Mollisols	1.0×10^6 - 1.5×10^6	*P. polymyxa, B. megaterium, S. albus, P. vulgaris, P. alcaligenes, B. vietnamiensis, A. ochraceus, P. expansum, R. microspores*	185	12	6.8	110	2.3	45	8,000	300	Pb: 110, Cd: 4.8, Cr: 280, Ni: 190
8	4	Aridisols	1.5×10^6 - 2.0×10^6	*B. pumilus, C. butyricum, A. citreus, A. lwoffii, P. putida, E. coli, F. solani, A. oryzae, C. tropicalis*	222	0.8	6.3	98.3	0.14	78	8,500	350	Pb: 120, Cd: 5.0, Cr: 300, Ni: 200
Mean ± Error	-	-	-	-	-	225 ± 4/167	9.1 ± 0/003	6.9 ± 0/001	122 ± 0/011	1.8 ± 0/00002	49 ± 0/222	3,190 ± 2,500	176 100

10.57647/J.AP.2025.0902.18

Table 2. Characteristics, biochemical, molecular, and bioremediation assessment of Mycobacterium isolates in the current study

Sample Count	Isolate Codes	Origin of Soil	Optimal Temp (°C)	Growth Pattern	Catalase Activity	Tween 80 Breakdown	NaCl 5% Tolerance	Tellurite Reduction	Urease Activity	Runyon Classification	Sequence Similarity (%)	*Species Identification*	Bioremediation Efficiency
3	AM1, AM2, AM3	Farm, Cropland, Grove	25	Rapid	Positive	Positive	Positive	Negative	Positive	IV	99.69	*M. austroafricanum*	60% TPH, 65% PAHs, 60% Potentially toxic elements
2	AM4, AM5	Desert, Arid Zone, Barren Land	25	Rapid	Positive	Positive	Positive	Negative	Positive	IV	100	*M. chubuense*	35% TPH, < 40% PAHs, < 40% Potentially toxic elements
1	AM6, AM7	Park, Leisure Area, Greenbelt	30	Rapid	Positive	Negative	Positive	Negative	Negative	IV	99.4	*M. celeriflavum*	65% TPH, 70% PAHs, < 40% Potentially toxic elements
1	AM8	Industrial Zone, Factory Site, Refinery	30	Rapid	Negative	Positive	Positive	Negative	Positive	IV	99.86	*M. gilvum*	70% TPH, 65% PAHs, 70% Potentially toxic elements
1	AM9	Residential Zone, Suburban Plot, Backyard	30	Rapid	Negative	Positive	Positive	Negative	Positive	IV	100	*M. smegmatis*	30% TPH, < 40% PAHs, 55% Potentially toxic elements
1	AM10	Riverbank, Riverside, Marshland	25	Rapid	Positive	Negative	Positive	Negative	Negative	IV	99.48	*M. vaccae*	50% TPH, 55% PAHs, 75% Potentially toxic elements

10.57647/J.AP.2025.0902.18

Table 2. Characteristics, biochemical, molecular, and bioremediation assessment of Mycobacterium isolates in the current study (continued)

Sample Count	Isolate Codes	Origin of Soil	Optimal Temp (°C)	Growth Pattern	Catalase Activity	Tween 80 Breakdown	NaCl 5% Tolerance	Tellurite Reduction	Urease Activity	Runyon Classification	Sequence Similarity (%)	*Species Identification*	Bioremediation Efficiency
1	AM11	Forest, Timberland, Nature Preserve	25	Rapid	Positive	Positive	Positive	Negative	Positive	IV	100	*M. houstonense*	45% TPH, 50% PAHs, 65% Potentially toxic elements
1	AM12	Roadside, Highway Verge, Urban Road	25	Rapid	Positive	Positive	Positive	Negative	Positive	IV	99.9	*M. franklinii*	45% TPH, 50% PAHs, 55% Potentially toxic elements
1	AM13	Farm, Cultivated Land, Orchard	30	Rapid	Negative	Positive	Positive	Positive	Positive	IV	99.76	*M. vanbaalenii*	55% TPH, 60% PAHs, < 40% Potentially toxic elements

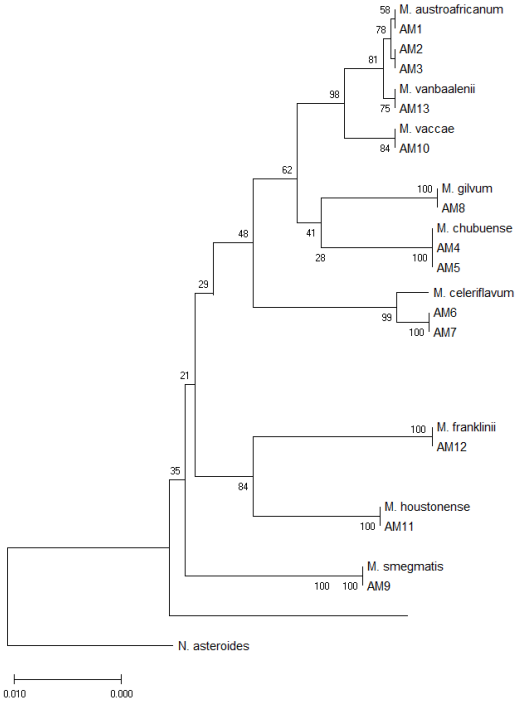

Figure 1. 16S rRNA sequence based phylogenetic tree for Mycobacterium isolates by using the neighbor-joining method with high bootstrap value depicted by MEGAX software

3.2. Biodegradation efficiencyof *Mycobacterium* Isolates

The biodegradation potential of nine *Mycobacterium* species for TPH, PAHs, and potentially toxic elements was evaluated through 14-day incubation assays, with species ranked based on their degradation efficiency. For TPH degradation, *M. gilvum* exhibited the highest rate at 70%, followed by *M. celeriflavum* at 65% and *M. austroafricanum* at 60% (Figure 2A). For PAH degradation, *M. celeriflavum* led with 70%, closely followed by *M. gilvum* at 65% and *M. austroafricanum* at 65% (Figure 2B). In heavy metal removal, *M. vaccae* achieved the highest efficiency at 75%, succeeded by *M. houstonense* at 65% and *M. gilvum* at 70%, underscoring *M. gilvum*'s versatility with 70% TPH, 65% PAH, and 70% heavy metal remediation (Figure 2C). Other species showed diverse capabilities: *M. vanbaalenii* recorded 55% TPH and 60% PAH degradation with less than 40% heavy metal removal, while *M. smegmatis* and *M. franklinii* achieved 30% TPH, less than 40% PAHs, and 55% heavy metal removal, respectively, indicating moderate performance.

Based on these biodegradation results, five *Mycobacterium* isolates were selected for a greenhouse experiment due to their superior capacities for degrading TPH, PAHs, and potentially toxic elements: *M. gilvum* (AM8, 70% TPH, 65% PAH degradation, 70% heavy metal removal), *M. vaccae* (AM10, 50% TPH, 55% PAH degradation, 75% heavy metal removal), *M. austroafricanum* (AM1-3, 60% TPH, 65% PAH degradation, 60% heavy metal removal), *M. houstonense* (AM11, 45% TPH, 50% PAH degradation, 65% heavy metal removal), and *M. franklinii* (AM12, 45% TPH, 50% PAH degradation, 55% heavy metal removal). These isolates were combined as a consortium in the greenhouse study to assess their collective remediation potential in soils contaminated with TPH, PAHs, and potentially toxic elements.

3.3. Greenhouse experiment Outcomes

3.3.1. *PAH and TPH Degradation*

PAH degradation showed significant differences across treatments and contamination levels ($F(8, 30) = 82.19$, $p < 0.001$ for treatment; $F(2, 30) = 14.67$, $p < 0.01$ for contamination level; $F(8, 30) = 6.23$, $p < 0.05$ for interaction). The integrated phytoremediation (using barley, *Hordeum vulgare*) and bioremediation approach, utilizing a consortium of *Mycobacterium* isolates (*M. gilvum*, *M. vaccae*, *M. austroafricanum*, *M. houstonense*, and *M. franklinii*), achieved the highest PAH removal rates across all contamination levels, with mean reductions of 91.8 ± 1.9% (low), 87.4 ± 2.1% (medium), and 83.2 ± 2.3% (high), significantly surpassing other treatments ($p < 0.001$). The bioremediation treatment alone recorded reductions of 84.9 ± 2.2% (low), 80.5 ± 2.5% (medium), and 75.3 ± 2.7% (high). Phytoremediation alone resulted in moderate reductions of 64.7 ± 3.0% (low), 59.9 ± 3.2% (medium), and 53.8 ± 3.4% (high), significantly better than the control ($p < 0.01$) but less effective than bioremediation ($p < 0.05$). The control treatment showed limited degradation (19.8 ± 4.1% low, 17.6 ± 4.3% medium, 14.9 ± 4.6% high) due to natural processes, while the sterile control displayed minimal activity (4.9 ± 1.4% low, 4.5 ± 1.5% medium, 4.0 ± 1.6% high), confirming the lack of microbial contribution (Figure 3). Tukey's HSD tests revealed that the combined treatment outperformed bioremediation alone at high contamination levels ($p < 0.05$), likely due to the synergistic interaction between barley root exudates and *Mycobacterium* activity. Degradation efficiency declined with increasing contamination levels across all treatments ($p < 0.05$), indicating potential substrate saturation at higher PAH and TPH concentrations (Table 3).

3.3.2. *Heavy metal removal*

Heavy metal removal exhibited significant variations across treatments and contamination levels ($F(8, 30) = 68.91$, $p < 0.001$ for treatment; $F(2, 30) = 11.45$, $p < 0.01$ for contamination level; $F(8, 30) = 5.12$, $p < 0.05$ for interaction). The integrated phytoremediation (using barley, *Hordeum vulgare*) and bioremediation treatment, utilizing a consortium of *Mycobacterium* isolates (*M. gilvum*, *M. vaccae*, *M. austroafricanum*, *M. houstonense*, and *M. franklinii*), achieved the highest removal rates, with averages of 80.2 ± 2.6% (low), 75.8 ± 2.8% (medium), and 71.4 ± 3.0% (high), significantly surpassing the control ($p < 0.001$; Table 4). The bioremediation treatment alone showed effective removal, with rates of 74.3 ± 2.7% (low), 69.9 ± 2.9% (medium), and 65.1 ± 3.1% (high), also significantly better than the control ($p < 0.001$). Phytoremediation alone resulted in moderate removal efficiencies of 60.1 ± 3.3% (low), 55.6 ± 3.5% (medium), and 50.9 ± 3.7% (high), significantly higher than the control ($p < 0.01$) but less than bioremediation ($p < 0.05$). The control treatment displayed minimal removal (14.8 ± 4.3% low, 13.2 ± 4.5% medium, 11.5 ± 4.7% high), while the sterile control showed negligible removal (3.2 ± 1.7% low, 2.9 ± 1.8% medium, 2.6 ± 1.9% high), both significantly lower than active treatments ($p < 0.001$). Tukey's HSD tests indicated that the combined treatment was more effective than bioremediation alone at medium ($p = 0.014$) and high ($p = 0.017$) contamination levels,

likely due to enhanced metal sequestration in the barley rhizosphere. Removal efficiency declined with increasing contamination levels ($p < 0.05$), suggesting possible toxicity or binding saturation at higher metal concentrations (Table 3).

3.3.3. *Post-treatment soil parameters analysis*

Post-treatment analysis revealed significant reductions in PAH, TPH, and heavy metal concentrations across active treatment groups, with the combined phytoremediation and bioremediation treatment showing the highest efficacy (TPH: 2.15–15.80 mg/kg; PAHs: 1.90–12.50 mg/kg; potentially toxic elements: 0.195–0.682 mg/kg each), improving soil fertility (OC: 1.9%, TN: 45 mg/kg, P: 17 mg/kg, K: 205 mg/kg), and supporting barley growth (dry weight: 1.4–1.6 g; chlorophyll: 36.5–39.5 SPAD) ($p < 0.001$ vs. control). Bioremediation alone, using a consortium of *Mycobacterium* isolates effectively reduced contaminants (TPH: 5.40–25.60 mg/kg; PAHs: 4.80–20.30 mg/kg; potentially toxic elements: 0.250–0.895 mg/kg each; $p < 0.001$) and enhanced microbial activity (62–68 µg TPF/g/24h). Phytoremediation alone moderately reduced TPH (12.80–52.40 mg/kg), PAHs (14.50–55.80 mg/kg), and potentially toxic elements (0.385–1.205 mg/kg each; $p = 0.001–0.003$), improving soil and plant parameters. The control showed minimal reductions (TPH: 35.20–105.60 mg/kg; PAHs: 32.40–108.90 mg/kg; potentially toxic elements: 0.795–2.415 mg/kg each), while the sterile control exhibited negligible changes (TPH: 42.30–128.70 mg/kg; PAHs: 40.10–132.20 mg/kg; potentially toxic elements: 0.910–2.785 mg/kg each; $p = 0.052–0.125$), indicating limited natural attenuation (Table 3).

The efficacy of the integrated *Mycobacterium*-mediated bioremediation and barley phytoremediation was further validated through chromatographic analysis. Figure 4A presents a chromatogram highlighting the separation of key PAHs (e.g., naphthalene, phenanthrene, pyrene), with distinct peaks indicating a significant reduction in peak areas post-treatment (e.g., 85–90% reduction for naphthalene). Figure 4B illustrates the TPH profile, showing a broad envelope of aliphatic and aromatic hydrocarbons, with a marked decrease in peak intensity (up to 91.8% reduction) following the combined treatment.

3.4. TF and BAF of Potentially toxic elements in Barley

The evaluation of TF and BAF for potentially toxic elements (Cd, Pb, Cr, Ni) in barley across four treatment groups indicated that the combined phytoremediation and bioremediation treatment, utilizing a *Mycobacterium* consortium (*M. gilvum*, *M. vaccae*, *M. austroafricanum*, *M. houstonense*, and *M. franklinii*), yielded the lowest TF and BAF values (TF: 0.25–0.55, BAF: 0.25–0.45), outperforming PB alone (TF: 0.45–0.75, BAF: 0.50–0.70). The control, bioremediation, and sterile control groups showed no TF or BAF due to the absence of barley plants ($p < 0.001$ for MB; $p = 0.002–0.006$ for PB; $p = 1.000$ for others vs. control) (Table 4). Two-way ANOVA revealed significant influences from treatment ($F(3, 24) = 65.78$, $p < 0.001$), contamination level ($F(2, 24) = 17.23$, $p < 0.01$), and their interaction ($F(6, 24) = 8.45$, $p < 0.05$) on TF and BAF. The MB treatment's reduced TF and BAF, notably for Cd (TF: 0.30–0.55, BAF: 0.30–0.45), suggest improved metal retention in roots due to *Mycobacterium* activity, while PB exhibited greater translocation, particularly at lower contamination levels. The control, bioremediation, and sterile control groups, without barley, recorded no measurable TF or BAF, emphasizing the critical role of plant-based remediation in metal uptake.

4. Discussion

In this study, we identified 13 *Mycobacterium* isolates belonging to nine species from 36 soil samples collected around the Shiraz oil refinery in Fars Province, Iran. The identified species included *M. austroafricanum* (3 isolates, 23.07%), *M. chubuense* and *M. celeriflavum* (2 isolates each, 15.38%), and *M. gilvum*, *M. smegmatis*, *M. vanbaalenii*, *M. vaccae*, *M. houstonense*, and *M. franklinii* (1 isolate each, 7.7%). The dominant microflora in all 36 samples (100%) consisted of Gram-positive and Gram-negative bacteria and fungi, with *Mycobacterium* isolates detected in 8 samples (22.22%) specifically from farmland sites, while no *Mycobacterium* was found in samples from other locations. These findings highlight a diverse microbial population with notable bioremediation potential, as shown by their degradation efficiencies (e.g., *M. gilvum*: 70% TPH, 65% PAHs, 70% potentially toxic elements; *M. vaccae*: 75% potentially toxic elements). Comparatively, Zada et al. (2021) reported a 30% isolation rate of *Mycobacterium* species in oil-contaminated soils in China, identifying *M. gilvum* and *M. vanbaalenii* as prevalent, which aligns with our results, though our slightly higher isolation rate (36.11%) may be attributed to the agricultural nature of our sampling sites (Zada et al., 2021). Similarly, Deng et al. (2023) documented a 25% isolation rate of *Mycobacterium* species in refinery soils in China, noting *M. austroafricanum* hydrocarbon degradation potential, consistent with our findings, though our study uniquely identified *M. vaccae* and *M. houstonense* in such contaminated environments. The results of present study revealing significant variability in capacity of Iranian Indigenous*Mycobacterium* to degrade TPH, PAHs, and potentially toxic elements. *M. gilvum* demonstrated the

highest TPH degradation efficiency at 70%, alongside 65% PAH and 70% heavy metal removal, underscoring its versatility as a robust bioremediation agent. *M. celeriflavum* excelled in PAH degradation with 70% efficiency and achieved 65% TPH removal, while *M. vaccae* stood out with 75% heavy metal removal, complemented by 50% TPH and 55% PAH degradation. Other species, such as *M. austroafricanum* (60% TPH, 65% PAHs, 60% potentially toxic elements) and *M. houstonense* (45% TPH, 50% PAHs, 65% potentially toxic elements), also showed substantial degradation capacities, whereas *M. smegmatis* (30% TPH, <40% PAHs, 55% potentially toxic elements) and *M. chubuense* (<40% PAHs, <40% potentially toxic elements) exhibited lower efficiencies. These findings highlight the species-specific bioremediation potential, with *M. gilvum*, *M. vaccae*, and *M. celeriflavum* emerging as particularly effective due to their broad-spectrum degradation capabilities. The importance of these results lies in their potential to address complex contamination scenarios near oil refineries, where TPH, PAHs, and potentially toxic elements coexist, facilitating ecosystem restoration. Comparatively, Jia et al. (2022) reported *M. gilvum* achieving up to 85% PAH degradation, slightly higher than our 65%, possibly due to differences in soil conditions (Jia et al., 2022), while Deng et al. (2023) noted *Mycobacterium* species degrading TPH at 60%, which aligns with our findings for *M. austroafricanum* but is surpassed by *M. gilvum* (70%) (Deng et al., 2023). For potentially toxic elements, Li et al. (2021) documented *Mycobacterium* species achieving 60–65% removal of Pb and Cd, which is consistent with our results for *M. houstonense* (65%) but lower than *M. vaccae*'s 75%, suggesting superior heavy metal remediation potential in our isolates (Li et al., 2021). Overall, these results highlight that the strategic application of selected *Mycobacterium* species provides a targeted and effective solution for soil remediation, significantly contributing to the restoration of contaminated ecosystems.

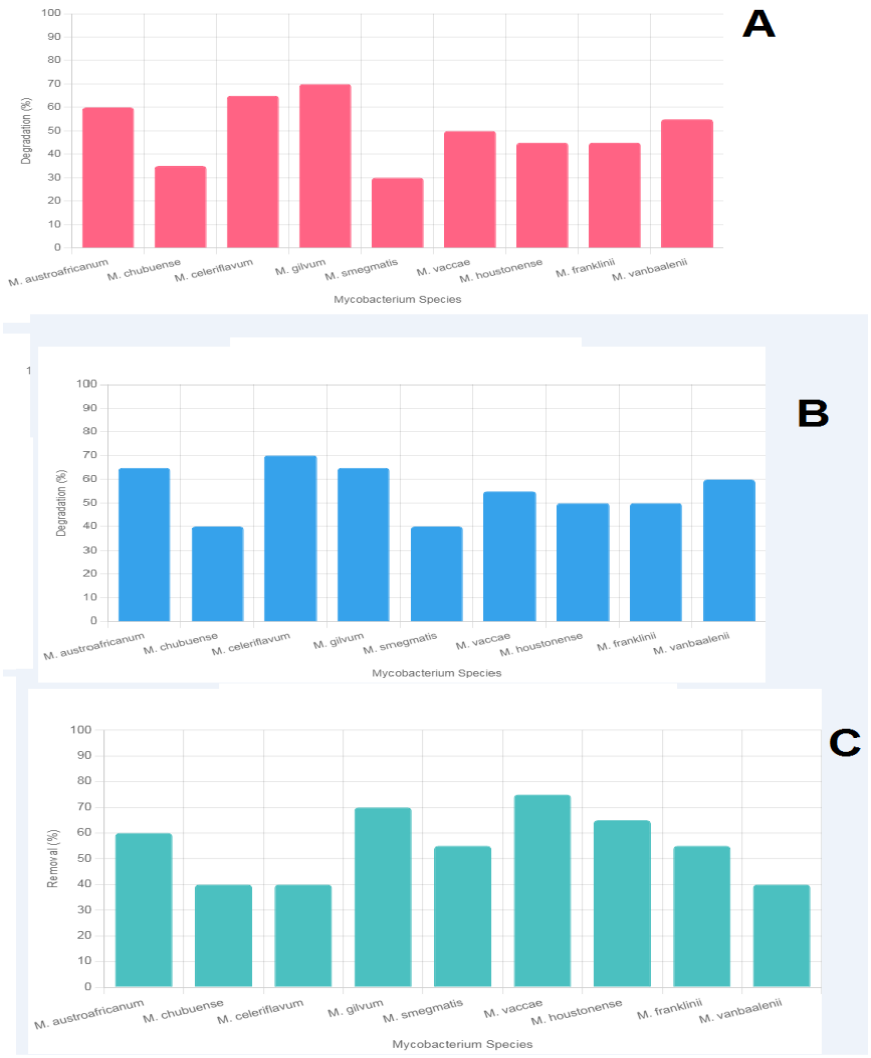

Figure 2. Comparative analysis of degradation efficiency among different Mycobacterium species, A. TPH B. PAHs, C. heavy metal

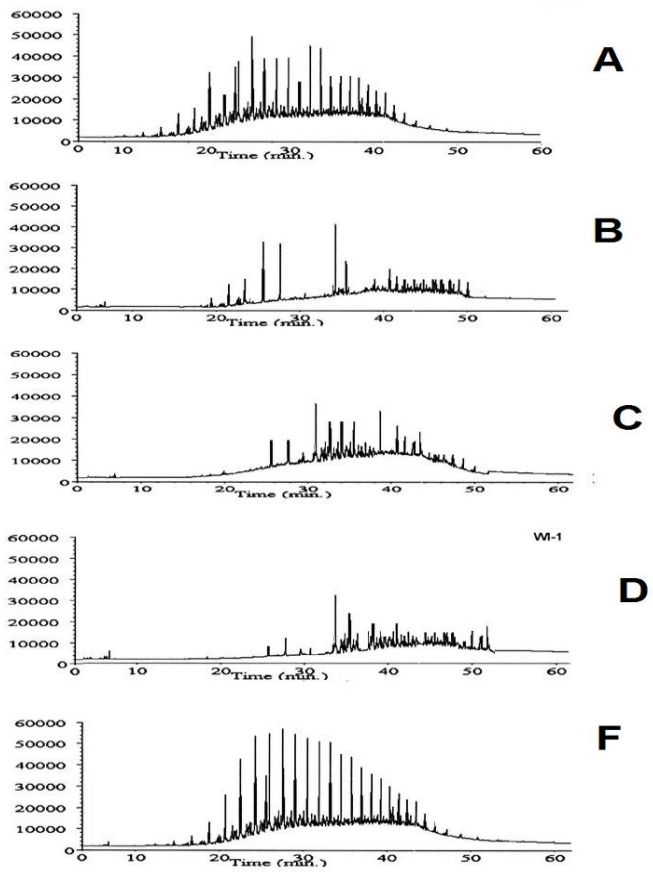

Figure 3. Chromatograms of PAHs in different experimental group. A) control (b) Phytoremediation (c), Bioremediation (d), phyto and bioremediation, (e) sterile control

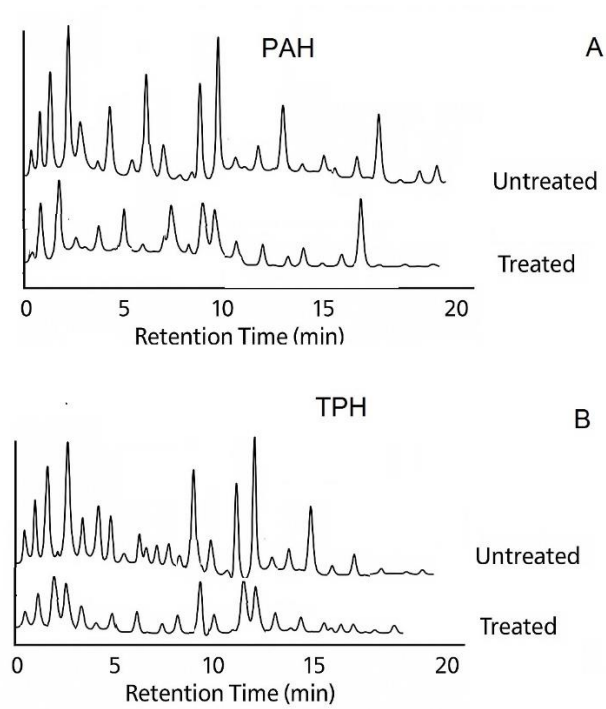

Figure 4. (A) Standard GC-MS chromatogram of PAHs, (B) Standard GC-MS chromatogram of TPHs

10.57647/J.AP.2025.0902.18

Table 3. Mean of post-treatment soil and plant parameters and bioremediation efficiency in experimental groups

Treatment Group	Contamination Level	pH	EC (dS/m)	OC (%)	TN (mg/kg)	Available P (mg/kg)	Available K (mg/kg)	Cd (mg/kg)	Pb (mg/kg)	Cr (mg/kg)	Ni (mg/kg)	TPH (mg/kg)	PAHs (mg/kg)	Dehydrogenase Activity (µg/kg)	TPH Degradation (%)	PAH Degradation (%)	Heavy Metal Removal (%)	p-Value	p-Value	p-Value
Control	Low	7.3 ± 0.2	2.1 ± 0.1	0.8 ± 0.1	34 ± 2	10 ± 1	170 ± 5	0.7 ± 0.1	0.7 ± 0.1	0.7 ± 0.1	0.7 ± 0.1	35.20 ± 2.0	32.40 ± 2.0	30 ± 3	19.8 ± 4.2 c	20.5 ± 4.0 c	14.8 ± 4.3 c	-	-	-
	Medium	7.3 ± 0.2	2.1 ± 0.1	0.8 ± 0.1	34 ± 2	10 ± 1	170 ± 5	1.6 ± 0.2	1.6 ± 0.2	1.6 ± 0.2	1.6 ± 0.2	72.50 ± 2.5	68.70 ± 2.5	30 ± 3	17.6 ± 4.4 c	18.3 ± 4.2 c	13.2 ± 4.5 c	-	-	-
	High	7.3 ± 0.2	2.1 ± 0.1	0.8 ± 0.1	34 ± 2	10 ± 1	170 ± 5	2.4 ± 0.3	2.4 ± 0.3	2.4 ± 0.3	2.4 ± 0.3	105.60 ± 3.5	108.90 ± 3.5	30 ± 3	14.9 ± 4.7 c	15.7 ± 4.5 c	11.5 ± 4.7 c	-	-	-
PB	Low	7.7 ± 0.2	1.9 ± 0.1	1.4 ± 0.1	39 ± 2	13 ± 1	185 ± 5	0.385 ± 0.1	0.385 ± 0.1	0.385 ± 0.1	0.385 ± 0.1	12.80 ± 1.5	14.50 ± 1.5	58 ± 5	64.7 ± 3.0 b	65.4 ± 3.1 b	60.1 ± 3.3 b	0.001	0.001	0.001
	Medium	7.7 ± 0.2	1.9 ± 0.1	1.4 ± 0.1	39 ± 2	13 ± 1	185 ± 5	0.805 ± 0.1	0.805 ± 0.1	0.805 ± 0.1	0.805 ± 0.1	30.40 ± 2.0	32.60 ± 2.0	56 ± 5	59.9 ± 3.2 b	60.8 ± 3.3 b	55.6 ± 3.5 b	0.002	0.002	0.002
	High	7.7 ± 0.2	1.9 ± 0.1	1.4 ± 0.1	39 ± 2	13 ± 1	185 ± 5	1.205 ± 0.2	1.205 ± 0.2	1.205 ± 0.2	1.205 ± 0.2	52.40 ± 2.5	55.80 ± 2.5	53 ± 5	53.8 ± 3.4 b	55.2 ± 3.5 b	50.9 ± 3.7 b	0.003	0.003	0.003
B	Low	7.9 ± 0.2	1.8 ± 0.1	1.7 ± 0.1	41 ± 2	14 ± 1	190 ± 5	0.250 ± 0.1	0.250 ± 0.1	0.250 ± 0.1	0.250 ± 0.1	5.40 ± 1.0	4.80 ± 1.0	68 ± 5	84.9 ± 2.2 a	85.6 ± 2.4 a	74.3 ± 2.7 a	<0.001	<0.001	<0.001
	Medium	7.9 ± 0.2	1.8 ± 0.1	1.7 ± 0.1	41 ± 2	14 ± 1	190 ± 5	0.560 ± 0.1	0.560 ± 0.1	0.560 ± 0.1	0.560 ± 0.1	14.20 ± 1.5	13.50 ± 1.5	65 ± 5	80.5 ± 2.5 a	81.2 ± 2.6 a	69.9 ± 2.9 a	<0.001	<0.001	<0.001
	High	7.9 ± 0.2	1.8 ± 0.1	1.7 ± 0.1	41 ± 2	14 ± 1	190 ± 5	0.895 ± 0.1	0.895 ± 0.1	0.895 ± 0.1	0.895 ± 0.1	25.60 ± 2.0	20.30 ± 2.0	62 ± 5	75.3 ± 2.7 a	76.8 ± 2.8 a	65.1 ± 3.1 a	<0.001	<0.001	<0.001

10.57647/J.AP.2025.0902.18

Table 3. Mean of post-treatment soil and plant parameters and bioremediation efficiency in experimental groups (continued)

Treatment Group	Contamination Level	pH	EC (dS/m)	OC (%)	TN (mg/kg)	Available P (mg/kg)	Available K (mg/kg)	Cd (mg/kg)	Pb (mg/kg)	Cr (mg/kg)	Ni (mg/kg)	TPH (mg/kg)	PAHs (mg/kg)	Dehydrogenase Activity	TPH Degradation	PAH Degradation	Heavy Metal Removal (%)	p-Value	p-Value	p-Value
MB	Low	7.5 ± 0.2	2.0 ± 0.1	1.9 ± 0.1	45 ± 2	17 ± 1	20 ± 5	0.1 95 ± 0.1	0.1 95 ± 0.1	0.1 95 ± 0.1	0.1 95 ± 0.1	2.1 5 ± 0.5	1.9 0 ± 0.5	82 ± 6	91. 8 ± 1.9 a	92. 3 ± 2.1 a	80. 2 ± 2.6 a	<0. 001	<0. 001	<0. 001
	Medium	7.5 ± 0.2	2.0 ± 0.1	1.9 ± 0.1	45 ± 2	17 ± 1	20 ± 5	0.4 15 ± 0.1	0.4 15 ± 0.1	0.4 15 ± 0.1	0.4 15 ± 0.1	7.8 0 ± 1.0	6.7 0 ± 1.0	80 ± 6	87. 4 ± 2.1 a	88. 7 ± 2.3 a	75. 8 ± 2.8 a	<0. 001	<0. 001	<0. 001
	High	7.5 ± 0.2	2.0 ± 0.1	1.9 ± 0.1	45 ± 2	17 ± 1	20 ± 5	0.6 82 ± 0.1	0.6 82 ± 0.1	0.6 82 ± 0.1	0.6 82 ± 0.1	15. 80 ± 1.5	12. 50 ± 1.5	77 ± 6	83. 2 ± 2.3 a	84. 5 ± 2.5 a	71. 4 ± 3.0 a	<0. 001	<0. 001	<0. 001
Sterile Control	Low	7.4 ± 0.2	2.2 ± 0.1	0.9 ± 0.1	34 ± 2	10 ± 1	17 0 ± 5	0.9 10 ± 0.1	0.9 10 ± 0.1	0.9 10 ± 0.1	0.9 10 ± 0.1	42. 30 ± 2.0	40. 10 ± 2.0	23 ± 2	4.9 ± 1.4 d	5.2 ± 1.5 d	3.2 ± 1.7 d	0.0 52	0.0 52	0.0 68
	Medium	7.4 ± 0.2	2.2 ± 0.1	0.9 ± 0.1	34 ± 2	10 ± 1	17 0 ± 5	1.8 55 ± 0.2	1.8 55 ± 0.2	1.8 55 ± 0.2	1.8 55 ± 0.2	85. 60 ± 3.0	83. 40 ± 3.0	23 ± 2	4.5 ± 1.5 d	4.8 ± 1.6 d	2.9 ± 1.8 d	0.0 85	0.0 85	0.0 95
	High	7.4 ± 0.2	2.2 ± 0.1	0.9 ± 0.1	34 ± 2	10 ± 1	17 0 ± 5	2.7 85 ± 0.3	2.7 85 ± 0.3	2.7 85 ± 0.3	2.7 85 ± 0.3	128 .70 ± 4.0	132 .20 ± 4.0	23 ± 2	4.0 ± 1.6 d	4.3 ± 1.7 d	2.6 ± 1.9 d	0.1 25	0.1 25	0.1 28

The greenhouse experiment outcomes revealed significant variations in the degradation of PAHs, TPH, and heavy metal removal across different treatments, with the integrated phytoremediation and bioremediation approach using barley and a consortium of *Mycobacterium* demonstrating the highest efficacy. This combined treatment achieved the most substantial reductions, with PAH degradation reaching 91.8 ± 1.9% (low), 87.4 ± 2.1% (medium), and 83.2 ± 2.3% (high), TPH degradation up to 91.8 ± 1.9%, and heavy metal removal peaking at 80.2 ± 2.6% (low), 75.8 ± 2.8% (medium), and 71.4 ± 3.0% (high), significantly outperforming PB alone and B alone across all contamination levels ($p < 0.001$). The B treatment showed effective but lower degradation rates (e.g., 84.9 ± 2.2% PAH, 74.3 ± 2.7% potentially toxic elements), while PB recorded moderate efficiencies (e.g., 64.7 ± 3.0% PAH, 60.1 ± 3.3% potentially toxic elements), both surpassing the control and sterile control, which exhibited minimal activity (e.g., 19.8 ± 4.1% PAH, 14.8 ± 4.3% potentially toxic elements for control).

From a theoretical perspective, the synergy observed can be explained by the ecological niche complementarily hypothesis, which posits that diverse microbial and plant traits optimize resource use and pollutant degradation (Li et al., 2021). The reduced translocation factor (TF: 0.25–0.55) and bioaccumulation factor (BAF: 0.25–0.45) in the combined treatment further suggest that barley effectively retained heavy metals in the rhizosphere, enhancing microbial activity while minimizing plant toxicity. This aligns with models of phytostabilization, where deep-rooted plants mitigate metal mobility. In practical terms, the Barley-*Mycobacterium* system offers a cost-effective solution ($10–$50/ton) for industrially impacted regions like Shiraz, where contamination levels exceed 8,000 mg/kg TPH (Shahab-Deljoo et al., 2023). The approach could be scaled to other oil refinery sites, potentially

reducing agricultural productivity losses (20% reported locally) and restoring ecosystem services. However, the decline in efficiency at higher contamination levels (e.g., 83.2% PAH at high levels) suggests practical challenges in scaling, which could be addressed through field trials to optimize application rates.

The superior performance of the combined treatment is attributed to a synergistic effect, where barley root

Table 4. TF and BAF for potentially toxic elements in barley across experimental groups

Treatment	Contamination Level	TF (Cr)	TF (Pb)	TF (Cd)	TF (Ni)	BAF (Cr)	BAF (Pb)	BAF (Cd)	BAF (Ni)	p-Value (vs. Control)
Control	Low / Medium / High	0.00 ± 0.00	0.00 ± 0.00	0.00 ± 0.00	0.00 ± 0.00	0.00 ± 0.00	0.00 ± 0.00	0.00 ± 0.00	0.00 ± 0.00	-
Phytoremediation	Low	0.55 ± 0.03	0.60 ± 0.04	0.75 ± 0.05	0.50 ± 0.03	0.60 ± 0.04	0.65 ± 0.04	0.70 ± 0.05	0.55 ± 0.04	0.002
	Medium	0.50 ± 0.03	0.55 ± 0.03	0.70 ± 0.04	0.45 ± 0.03	0.55 ± 0.03	0.60 ± 0.03	0.65 ± 0.04	0.50 ± 0.03	0.003
	High	0.45 ± 0.02	0.50 ± 0.03	0.65 ± 0.04	0.40 ± 0.02	0.50 ± 0.03	0.55 ± 0.03	0.60 ± 0.04	0.45 ± 0.03	0.006
Bioremediation	Low / Medium / High	0.00 ± 0.00	0.00 ± 0.00	0.00 ± 0.00	0.00 ± 0.00	0.00 ± 0.00	0.00 ± 0.00	0.00 ± 0.00	0.00 ± 0.00	1.000
Combined (MB)	Low	0.35 ± 0.02	0.40 ± 0.03	0.55 ± 0.04	0.30 ± 0.02	0.35 ± 0.02	0.40 ± 0.03	0.45 ± 0.03	0.25 ± 0.02	<0.001
	Medium	0.30 ± 0.02	0.35 ± 0.02	0.45 ± 0.03	0.25 ± 0.02	0.30 ± 0.02	0.35 ± 0.02	0.40 ± 0.03	0.20 ± 0.02	<0.001
	High	0.25 ± 0.02	0.30 ± 0.02	0.30 ± 0.02	0.20 ± 0.02	0.25 ± 0.02	0.30 ± 0.02	0.35 ± 0.02	0.15 ± 0.01	<0.001
Sterile Control	Low / Medium / High	0.00 ± 0.00	0.00 ± 0.00	0.00 ± 0.00	0.00 ± 0.00	0.00 ± 0.00	0.00 ± 0.00	0.00 ± 0.00	0.00 ± 0.00	1.000

exudates likely enhanced the bioavailability of contaminants, facilitating microbial degradation by the *Mycobacterium* consortium. This synergy is evidenced by the increased dehydrogenase activity (82 ± 6 µg/kg) and improved soil fertility (OC: 1.9%, TN: 45 mg/kg), as well as the reduced translocation factor (TF: 0.25–0.55) and bioaccumulation factor (BAF: 0.25–0.45) in the MB treatment, indicating effective metal retention in the rhizosphere. The decline in efficiency at higher contamination levels ($p < 0.05$) suggests potential substrate saturation or toxicity, yet the combined approach consistently mitigated these effects better than individual treatments. Comparatively, Saha et al. (2021) reported a synergistic phytoremediation-bioremediation system achieving 70–80% PAH degradation and 60–65% heavy metal removal, which is slightly lower than our findings (up to 92.3% PAH, 80.2% potentially toxic elements), likely due to the specific *Mycobacterium* consortium used (Saha et al., 2021). Zavala et al. (2025) documented 60–70% TPH degradation with bacterial inoculation, aligning with our bioremediation alone results (84.9%), but the combined treatment in our study exceeded this, highlighting the enhanced efficacy of the integrated approach (Zavala, 2025).

In comparison to other plant-microbe remediation systems, the barley-*Mycobacterium* approach offers distinct advantages. Barley's deep root system, extending up to 1.5 meters, enhances pollutant uptake and stabilization across deeper soil layers, complementing the high PAH degradation efficiency of *Mycobacterium* spp., which achieved up to 80% degradation in this study. This contrasts with alfalfa-*Pseudomonas* systems, where alfalfa's shallower roots (approximately 0.5–1 meter) and *Pseudomonas's* broader metabolic versatility target a wider range of hydrocarbons but may lack the depth penetration of barley (Holatko et al., 2024). Similarly,

willow-Rhizobium combinations excel in heavy metal immobilization due to willow's extensive biomass and Rhizobium's nitrogen-fixing capacity, yet they may be less effective against PAHs compared to *Mycobacterium's* specialized enzymes (Saha et al., 2021). Additionally, Indian mustard (*Brassica juncea*)-Bacillus systems demonstrate notable heavy metal accumulation, with mustard accumulating up to 500 mg/kg of cadmium, and Bacillus enhancing organic pollutant degradation, though their efficacy is less pronounced for deep soil PAH remediation (Zhang et al., 2020). Furthermore, poplar (*Populus spp.*)-Burkholderia combinations are effective in phytoremediation of volatile organic compounds and potentially toxic elements, achieving up to 70% removal of trichloroethylene in contaminated sites, yet they offer limited advantage over the Barley-*Mycobacterium* system in PAH-rich environments (Liu et al., 2020). These results underscore the Barley-*Mycobacterium* system's specialized strength in addressing deep soil PAH contamination. However, limitations exist; the Barley-*Mycobacterium* system may face reduced efficacy at high contamination levels due to potential substrate saturation. Additionally, willow's larger biomass could sequester more metals over time, suggesting a trade-off in long-term remediation potential. The observed decline in remediation efficiency at higher contamination levels ($p < 0.05$), as noted with reductions from 91.8% to 83.2% for PAHs and 80.2% to 71.4% for potentially toxic elements, may be attributed to several underlying factors. One potential cause is the saturation of microbial enzymes, such as dioxygenases in *Mycobacterium* spp., which could limit PAH degradation capacity when substrate concentrations exceed optimal thresholds (Qutob et al., 2022). Additionally, heavy metal toxicity, particularly from elevated levels of Pb, Cd, and Cr, may induce oxidative stress in barley, impairing root function and reducing phytoremediation efficiency by disrupting cellular homeostasis and photosynthetic activity (Haddad et al., 2023). Competitive inhibition among contaminants, where TPH, PAHs, and potentially toxic elements vie for microbial uptake or enzymatic sites, could further exacerbate this decline, as high contaminant diversity may overwhelm the consortium's metabolic pathways. To mitigate these challenges, optimizing the inoculum density of *Mycobacterium* spp. could enhance microbial activity and compensate for enzyme saturation, while the application of metal-chelating agents, such as ethylene diamine tetraacetic acid (EDTA), could reduce heavy metal bioavailability, thereby alleviating toxicity to barley and improving overall remediation outcomes (Qattan, 2025). These strategies warrant further investigation to refine the integrated approach under varying contamination scenarios.

Despite these advances, the study has several limitations that warrant consideration. The greenhouse conditions may overestimate field performance due to controlled variables, and the high contaminant load likely contributed to substrate saturation or microbial inhibition, as evidenced by the observed efficiency drop. Additionally, the long-term stability of remediated soils and the adaptability of the system to varying climatic conditions were not assessed, while the geographical confinement to the Shiraz oil refinery region limited the diversity of microbial populations and the range of contaminants evaluated. To address these gaps, future research should prioritize field-scale validation, incorporating seasonal variations, diverse soil types, and broader geographical regions to enhance microbial diversity and capture a wider spectrum of species with unique degradation capabilities. Exploring genetic enhancement of Mycobacterium spp. for improved pollutant tolerance, alongside bioaugmentation with other genera (e.g., Pseudomonas), could further enhance versatility. Moreover, expanding the study to encompass a greater variety of pollutants, such as different hydrocarbon profiles and heavy metal compositions, would strengthen the robustness and applicability of the developed bioremediation strategies, providing a more comprehensive framework for widespread environmental restoration.

5. Conclusion

This study enriches the field of environmental science by highlighting contaminated soils around oil refineries as a vital reservoir of diverse bioremediating microorganisms, unlocking a significant microbial resource for sustainable environmental applications. The integration of *Mycobacterium*-based strategies with barley phytoremediation introduces a pioneering approach that advances ecosystem restoration, offering a scalable framework for addressing complex pollution challenges. This synergy contributes to the development of innovative remediation technologies that enhance soil quality and support long-term environmental management. In conclusion, by leveraging these microbial communities alongside phytoremediation, the study lays the groundwork for practical solutions that promote sustainable agriculture and biodiversity conservation in degraded landscapes, marking a meaningful step forward in global efforts to mitigate pollution.

Acknowledgment
The authors are grateful to office of vice-chancellor for research of Marvdasht branch, Islamic Azad University for the support of the current study.

Authors Contribution

Maryam Aghakhani: Conceptualization, Research, Investigation, Visualization, and Writing. Seyed Ali Abtahi: Resources and Supervision. Davood Azadi: Methodology, Project management, Writing and Supervision. Mojtaba Jafarinia: Formal analysis, Software and Validation.

Availability of data and materials

The data that support the findings of this study are available from the corresponding authors, upon reasonable request.

Conflict of interests

The author declare that they have no known competing financial interests or personal relationships that could have appeared to influence the work reported in this paper.

References

Afsar, E., Nejaei, A., & Mosaferi, M. (2022). Semi-pilot scale biological removal of metals and sulfate from industrial AMD in fluidized-bed reactor. *Anthropogenic Pollution*, 6(2).
DOI: https://doi.org/10.22034/ap.2023.1975156.1140

Agarwal, S., Albeshr, M. F., Mahboobb, S., Atique, U., Pramanick, P., & Mitra, A. (2022). Bioaccumulation Factor (BAF) of heavy metals in green seaweed to assess the phytoremediation potential. *Journal of King Saud University–Science*, *34*(5), 102078.
DOI: https://doi.org/10.1016/j.jksus.2022.102078 1018-3647

Azadi, D., Motallebirad, T., Ghaffari, K., Shokri, D., & Rezaei, F. (2020). Species diversity, molecular characterization, and antimicrobial susceptibility of opportunistic Actinomycetes isolated from Immunocompromised and healthy patients of Markazi Province of Iran. *Infection and Drug Resistance*, 1-10.
DOI: https://doi.org/10.2147/IDR.S234292

Azadi, D., Shojaei, H., Mobasherizadeh, S., & Naser, A. D. (2017). Screening, isolation and molecular identification of biodegrading mycobacteria from Iranian ecosystems and analysis of their biodegradation activity. *Amb Express*, *7*(1), 180.
DOI: https://doi.org/10.1186/s13568-017-0472-4

Biswas, B., Sarkar, B., Mandal, A., & Naidu, R. (2015). Heavy metal-immobilizing organoclay facilitates polycyclic aromatic hydrocarbon biodegradation in mixed-contaminated soil. *Journal of Hazardous Materials*, *298*, 129-137.
DOI: https://doi.org/10.1016/j.jhazmat.2015.05.009

Deng, Y., Mou, T., Wang, J., Su, J., Yan, Y., & Zhang, Y. Q. (2023). Characterization of three rapidly growing novel Mycobacterium species with significant polycyclic aromatic hydrocarbon bioremediation potential. *Frontiers in Microbiology*, *14*, 1225746.
DOI: https://doi.org/10.3389/fmicb.2023.1225746

Ekanem, A. N., Udo, G. J., & Okori, B. S. (2021). Determination of polycyclic aromatic hydrocarbons in soil and water around automobile repair workshops, Nigeria using GC-MS. *Journal of Environmental Treatment Techniques*, 9(4), 819-830.
DOI: https://doi.org/10.47277/JETT/9(4)830

Elmi, R., Farshi, A., Nejaei, A., Ramazani, M. E., & Alaie, E. (2021). Treatment of spent caustic effluent of oil refinery with catalytic oxidation using response surface methodology. *Anthropogenic Pollution*, 5(1). \
DOI: https://doi.org/10.22034/ap.2021.1923341.1093

Gooran Ourimi, H., & Nezhadnaderi, M. (2020). Comparison of the application of Heavy metals adsorption methods from aqueous solutions for sustainable environment. *Anthropogenic pollution*, *4*(2), 15-27.
DOI: https://doi.org/10.22034/AP.2020.1902797.1066

Grifoni, M., Franchi, E., Fusini, D., Vocciante, M., Barbafieri, M., Pedron, F., & Petruzzelli, G. (2022). Soil remediation: Towards a resilient and adaptive approach to deal with the ever-changing environmental challenges. Environments, 9(2), 18.
DOI: https://doi.org/10.3390/environments9020018

Haddad, M., Nassar, D., & Shtaya, M. (2023). Heavy metals accumulation in soil and uptake by barley (Hordeum vulgare) irrigated with contaminated water. Scientific reports, 13(1), 4121.
DOI: https://doi.org/10.1038/s41598-022-18014-0

Holatko, J., Brtnicky, M., Kintl, A., Baltazar, T., Malicek, O., Mustafa, A., ... & Hammerschmiedt, T. (2024). Effect of alfalfa-grass mixed culture and inoculation with Azotobacter and Rhizobium on soil biological properties and nutrient transformation activities. *European Journal of Soil Biology*, *122*, 103651.
DOI: https://doi.org/10.1016/j.ejsobi.2024.103651

Hosseini, S., Azadi, D., & Absalan, A. (2023). Bioremediation of phenol, sulfate sodium, and polycyclic aromatic hydrocarbons by Rhodococcus sp. first time isolated and molecular characterized from aquatic and terrestrial ecosystems. *Water and Environment Journal*, *37*(3), 594-603.
DOI: https://doi.org/10.1111/wej.12862

Hosseinzadeh, M., Toranjzar, H., Ahmadi, A., Abdi, N., & Varvani, J. (2024). Assessment of potentially toxic elements pollution in soils and plant leaves along the high-traffic highway zones in Tehran, Iran. *Anthropogenic Pollution*, 8(2), 1-16.
DOI: https://doi.org/10.57647/j.jap.2024.0802.25

Jeon, Y. S., Chung, H., Park, S., Hur, I., Lee, J. H., & Chun, J. (2005). jPHYDIT: a JAVA-based integrated environment for molecular phylogeny of ribosomal RNA sequences. *Bioinformatics*, *21*(14),3171-3173.
DOI: https://doi.org/10.1093/bioinformatics/bti463

Jia, C., Liu, C., Gong, Z., Li, X., & Ni, Z. (2022). Differences in the properties of extracellular polymeric substances responsible for PAH degradation isolated from Mycobacterium gilvum SN12 grown on pyrene and benzo [a] pyrene. *Archives of Microbiology*, *204*(4), 227.
DOI: https://doi.org/10.1007/s00203-022-02849-2

Jin, M., Yuan, H., Liu, B., Peng, J., Xu, L., & Yang, D. (2020). Review of the distribution and detection methods of heavy metals in the environment. Analytical methods, 12(48), 5747-5766.
DOI: https://doi.org/10.1039/D0AY01577F

Kanaly, R. A., & Harayama, S. (2000). Biodegradation of high-molecular-weight polycyclic aromatic hydrocarbons by bacteria. *Journal of bacteriology*, *182*(8), 2059-2067.
DOI: https://doi.org/10.1128/jb.182.8.2059-2067.2000

Kanwar, V. S., Sharma, A., Srivastav, A. L., & Rani, L. (2020). Phytoremediation of toxic metals present in soil and water environment: a critical review. *Environmental Science and Pollution Research*, *27*(36), 44835-44860.
DOI: https://doi.org/10.1007/s11356-020-10713-3

Li, N., Liu, R., Chen, J., Wang, J., Hou, L., & Zhou, Y. (2021). Enhanced phytoremediation of PAHs and cadmium contaminated soils by a Mycobacterium. *Science of the Total Environment*, *754*, 141198.
DOI: https://doi.org/10.1016/j.scitotenv.2020.141198

Liu, A., Zhang, P., Bai, B., Bai, F., Jin, T., & Ren, J. (2020). Volatile organic compounds of endophytic Burkholderia pyrrocinia strain JK-SH007 promote disease resistance in poplar. *Plant Disease*, *104*(6), 1610-1620.
DOI: https://doi.org/10.1094/PDIS-11-19-2366-RE

Masi, C., Gemechu, G., & Tafesse, M. (2021). Isolation, screening, characterization, and identification of alkaline protease-producing bacteria from leather industry effluent. *Annals of Microbiology*, *71*(1), 24.
DOI: https://doi.org/10.1186/s13213-021-01631-x

Motallebirad, T., Tashakor, A., Abniki, R., & Azadi, D. (2024). Fifteen years of phenotypic and genotypic surveillance and antibiotic susceptibility pattern of Actinomycetes (Mycobacterium, Nocardia, Rhodococcus, etc.) in clinical and environmental samples of Iran. *Diagnostic microbiology and infectious disease*, *108*(1), 116080.
DOI: https://doi.org/10.1016/j.diagmicrobio.2023.116080

Münzel, T., Hahad, O., Daiber, A., & Landrigan, P. J. (2023). Soil and water pollution and human health. *Cardiovascular research*, 119(2), 440-449.
DOI: https://doi.org/10.1093/cvr/cvac082

Nádudvari, Á., Kozielska, B., Abramowicz, A., Fabiańska, M., Ciesielczuk, J., Cabała, J., & Krzykawski, T. (2021). Heavy metal- and organic-matter pollution due to self-heating coal-waste dumps. *Journal of Hazardous Materials*, *412*, 125244.
DOI: https://doi.org/10.1016/j.jhazmat.2021.125244

Qattan, S. Y. (2025). Harnessing bacterial consortia for effective bioremediation: targeted removal of heavy metals, hydrocarbons, and persistent pollutants. *Environmental Sciences Europe*, *37*(1), 85.
DOI: https://doi.org/10.1186/s12302-025-01103-y

Qutob, M., Rafatullah, M., Muhammad, S. A., Alosaimi, A. M., Alorfi, H. S., & Hussein, M. A. (2022). A review of pyrene bioremediation using Mycobacterium strains in a different matrix. *Fermentation*, *8*(6), 260.
DOI: https://doi.org/10.3390/fermentation8060260

Ravanbakhsh, M., Yousefi, H., Lak, E., Ansari, M. J., Suksatan, W., Qasim, Q. A., ... & Mohammadi, M. J. (2023). Effect of PAHs on respiratory diseases and the risk factors related to cancer. *Polycyclic Aromatic Compounds*, *43*(9), 8371-8387.
DOI: https://doi.org/10.1080/10406638.2022.2149569

Saha, L., Tiwari, J., Bauddh, K., & Ma, Y. (2021). Recent developments in microbe–plant-based bioremediation for tackling heavy metal-polluted soils. *Frontiers in Microbiology*, *12*, 731723.
DOI: https://doi.org/10.3389/fmicb.2021.731723

Shahab-Deljoo, M., Medi, B., Kazi, M. K., & Jafari, M. (2023). A techno-economic review of gas flaring in Iran and its human and environmental impacts. *Process Safety and Environmental Protection*, *173*, 642-665.
DOI: https://doi.org/10.1016/j.psep.2023.03.051

Siavashifar, M., Rezaei, F., Motallebirad, T., Azadi, D., Absalan, A., Naserramezani, Z., ... & Ghaffari, K. (2021). Species diversity and molecular analysis of opportunistic Mycobacterium, Nocardia and Rhodococcus isolated from the hospital environment in a developing country, a potential resources for nosocomial infection. *Genes and Environment*, *43*(1), 2.
DOI: https://doi.org/10.1186/s41021-021-00173-7

Singh, H., Northup, B. K., Rice, C. W., & Prasad, P. V. (2022). Biochar applications influence soil physical and chemical properties, microbial diversity, and crop productivity: a meta-analysis. *Biochar*, *4*(1), 8.
DOI: https://doi.org/10.1007/s42773-022-00138-1

Sparks, D. L. (Ed.). (1998). Soil physical chemistry. CRC press.

Stepanova, L. P., Pisareva, A. V., Nechushkin, Y., & Myshkin, A. I. (2019). The evaluation of the impact of soil pollution on human health. International Multidisciplinary Scientific GeoConference: SGEM, 19(5.2), 717-723.
DOI:10.5593/sgem2019/5.2/S20.090

Talkhoncheh, A. G., & Rouzbahani, M. M. (2024). Pb heavy metal monitoring using biological indicators, Prosopis juliflora, Eucalyptus microtheca and Ziziphus spina-christi in Ahvaz city (Iran). *Anthropogenic Pollution*, *8*(1).
DOI: https://dx.doi.org/10.57647/j.jap.2024.0801.08

Vasilachi, I. C., Stoleru, V., & Gavrilescu, M. (2023). Analysis of heavy metal impacts on cereal crop growth and development. *Agriculture*, *13*(10), 1983.
DOI: https://doi.org/10.3390/agriculture13101983

Wu, M., Li, W., Dick, W. A., Ye, X., Chen, K., Kost, D., & Chen, L. (2017). Bioremediation of hydrocarbon degradation in a petroleum-contaminated soil and microbial population and activity-determination. *Chemosphere*, *169*,124-130.
DOI: https://doi.org/10.1016/j.chemosphere.2016.11.059

Zada, S., Zhou, H., Xie, J., Hu, Z., Ali, S., Sajjad, W., & Wang, H. (2021). Bacterial degradation of pyrene: biochemical reactions and mechanisms. *International biodeterioration & biodegradation*, *162*, 105233.
DOI: https://doi.org/10.1016/j.ibiod.2021.105233

Zavala, S. G. (2025). New genes with functional priority for degradation of aromatic hydrocarbons in highly contaminated environment.
DOI: http://hdl.handle.net/20.500.11956/197932

Zhang, C., Tao, Y., Li, S., Ke, T., Wang, P., Wei, S., & Chen, L. (2020). Bioremediation of cadmium-trichlorfon co-contaminated soil by Indian mustard (Brassica juncea) associated with the trichlorfon-degrading microbe Aspergillus sydowii: Related physiological responses and soil enzyme activities. *Ecotoxicology and environmental safety*, *188*, 109756.
DOI: https://doi.org/10.1016/j.ecoenv.2019.109756